Supporting Information for:

The Electronic and Solvatochromic Properties of $[Co(L)(bipyridine)_2]^+$ (L = *o*-catecholato, *o*-benzenedithiolato) Species: a Combined Experimental and Computational Study

Giacomo Cioncoloni, Hans M. Senn, Stephen Sproules, Claire Wilson and Mark D. Symes*

WestCHEM, School of Chemistry, University of Glasgow, University Avenue, Glasgow, G12 8QQ, UK.

*E-mail: mark.symes@glasgow.ac.uk

Index *Page*

^{1}H NMR spectrum, TGA analysis and PXRD of complex **1** S3

^{1}H NMR spectra, TGA analysis and PXRD of complex **2** S6

^{1}H NMR spectra and TGA analysis of complex **3** S10

EPR spectrum of complex **2** in acetonitrile/THF solution at 150 K S13

Supplementary computational methods and results S14

Figure **S12** S16

Figure **S13** S17

Figure **S14** S18

Figure **S15** S19

Figure **S16** S20

Crystallographic data S21

References S29

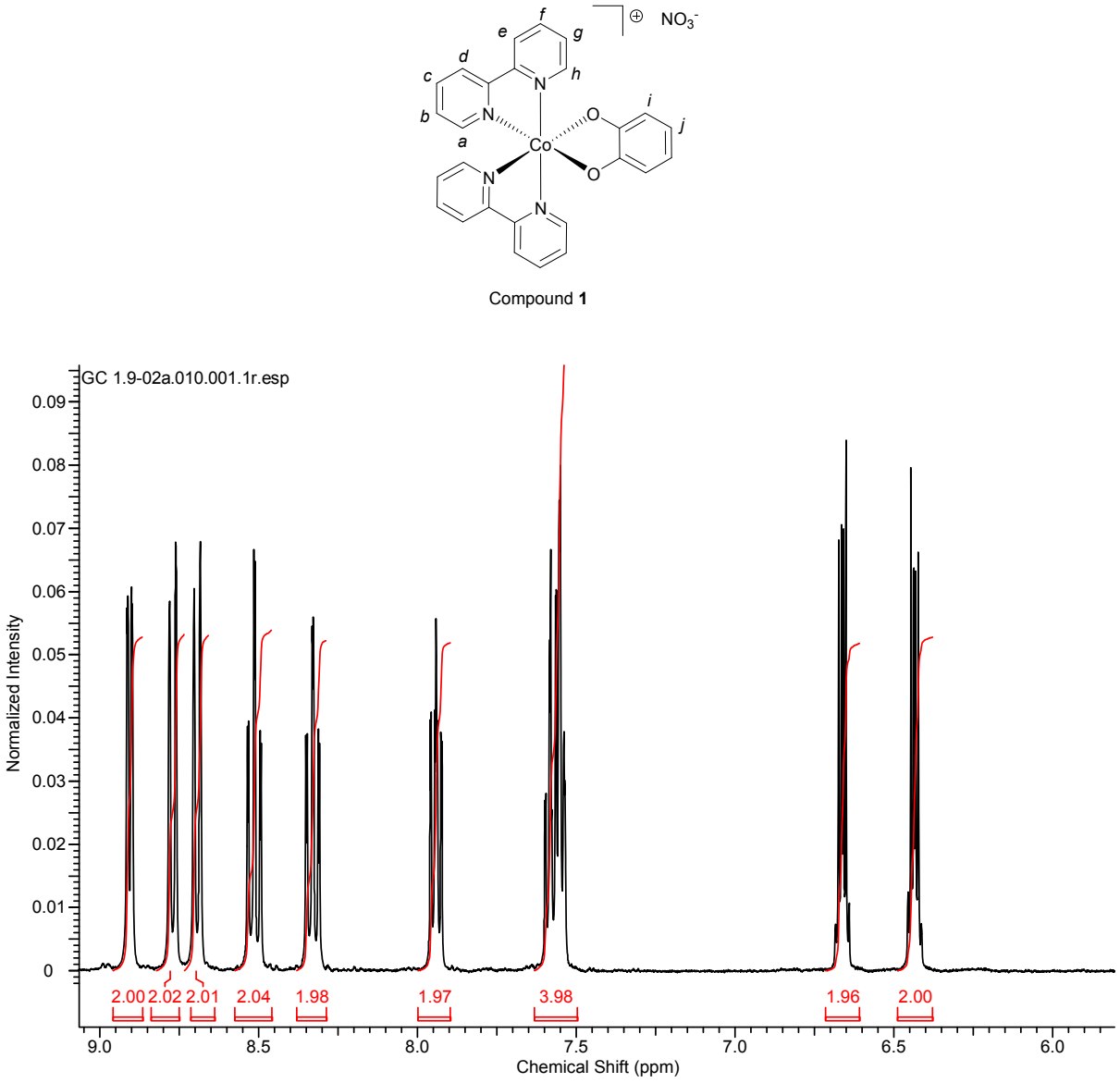

Figure S1. ^{1}H NMR spectrum of compound **1** in 90% MeOD / 10% D_2O.

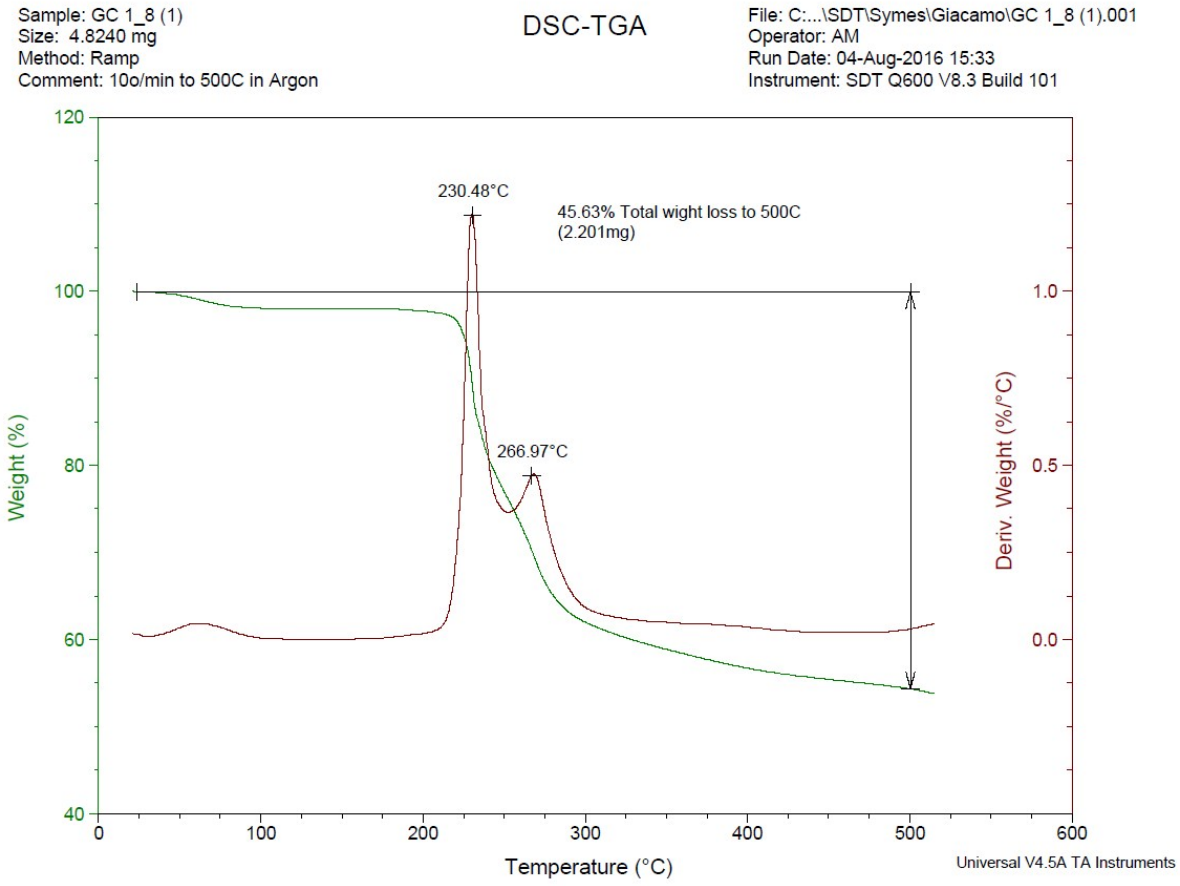

Figure S2. TGA analysis on compound **1**.

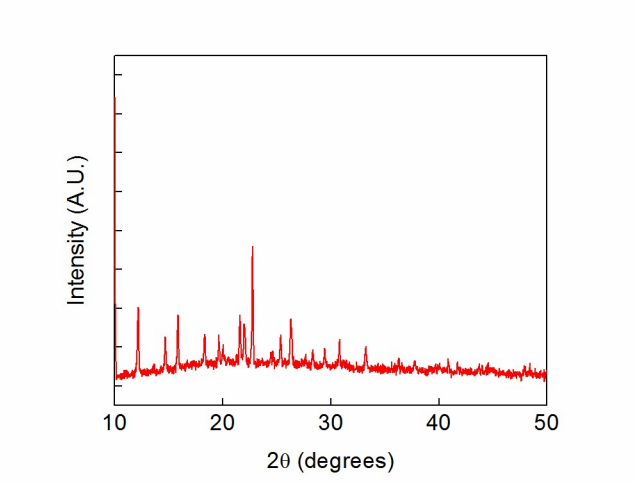

Figure S3. The PXRD pattern of compound **1**. A discussion comparing this pattern to that of compound **2** is given with Figure S7 (below).

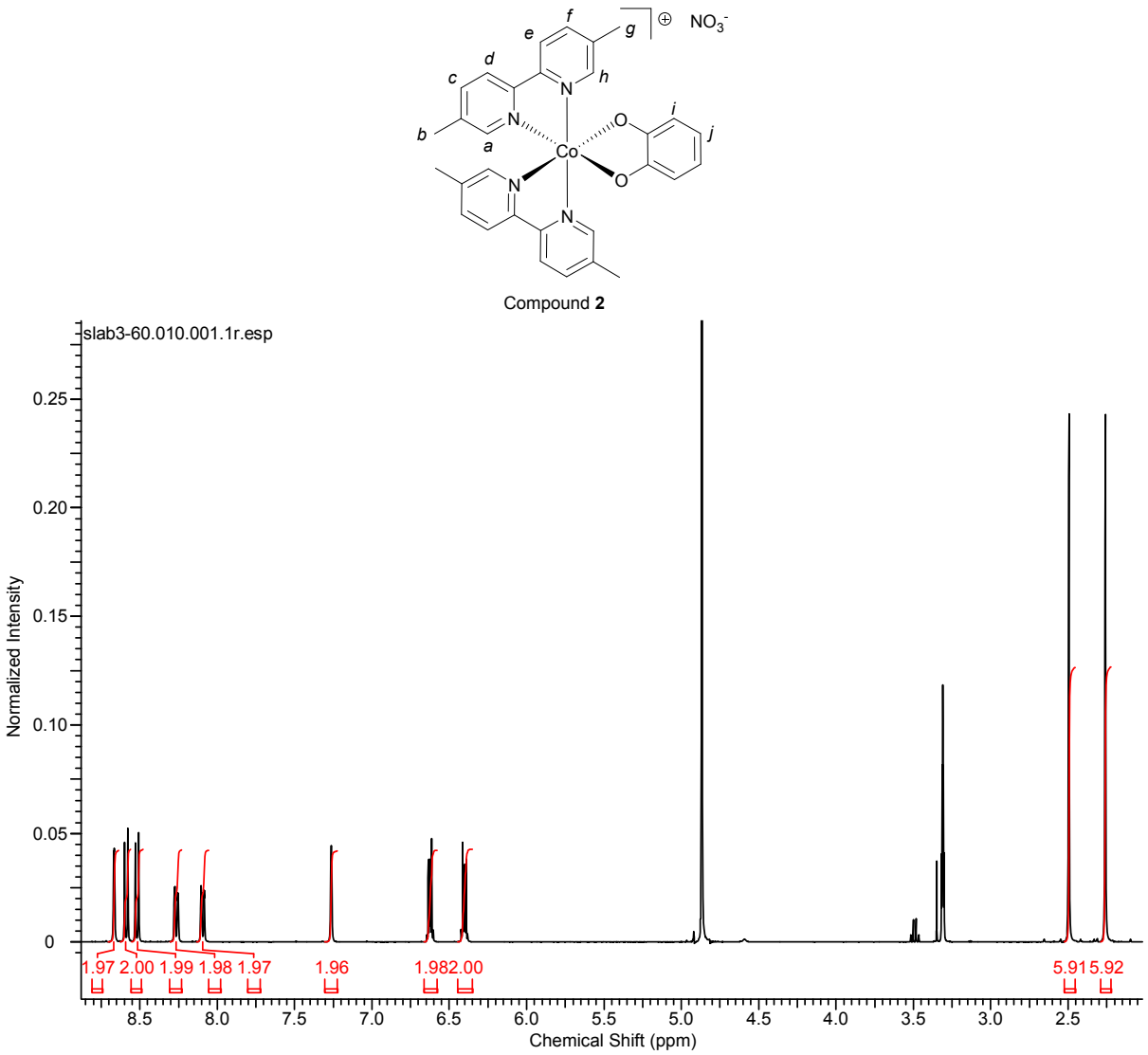

Figure S4. ^{1}H NMR spectrum of compound **2** in MeOD.

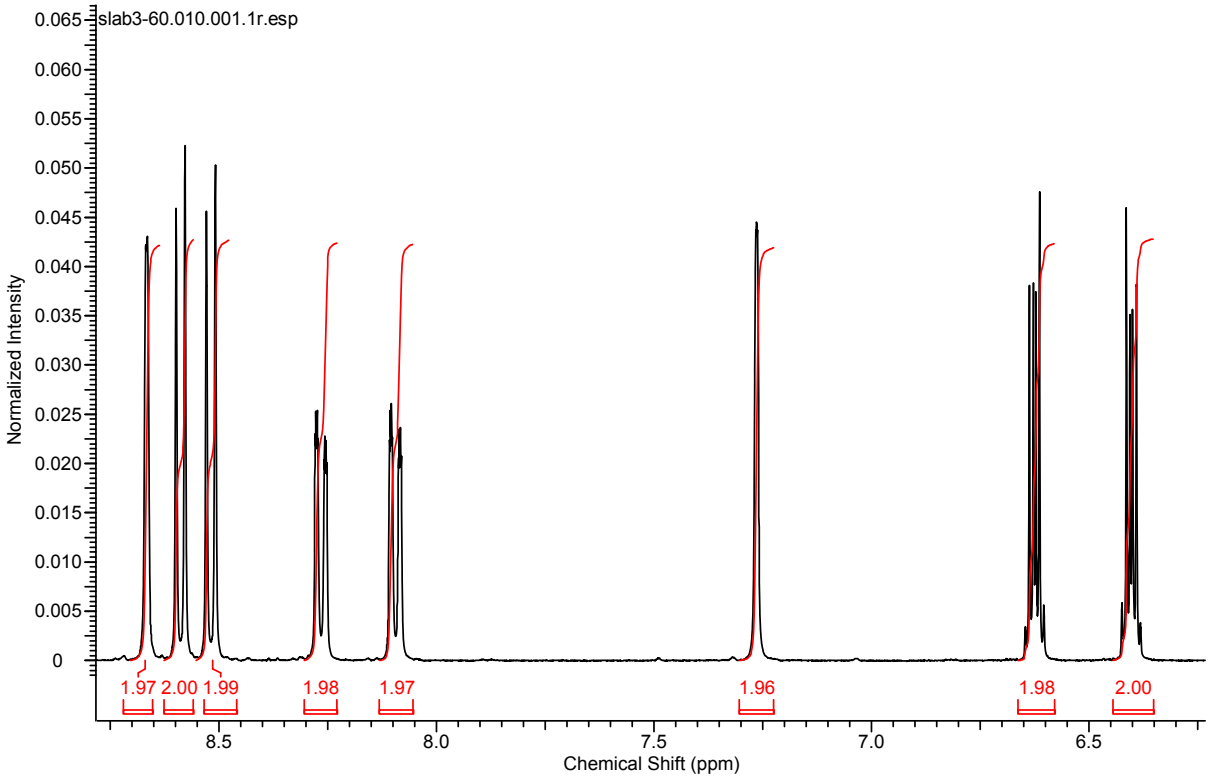

Figure S5. Expansion of the aromatic region of the ^{1}H NMR spectrum of **2** shown in Fig. S2.

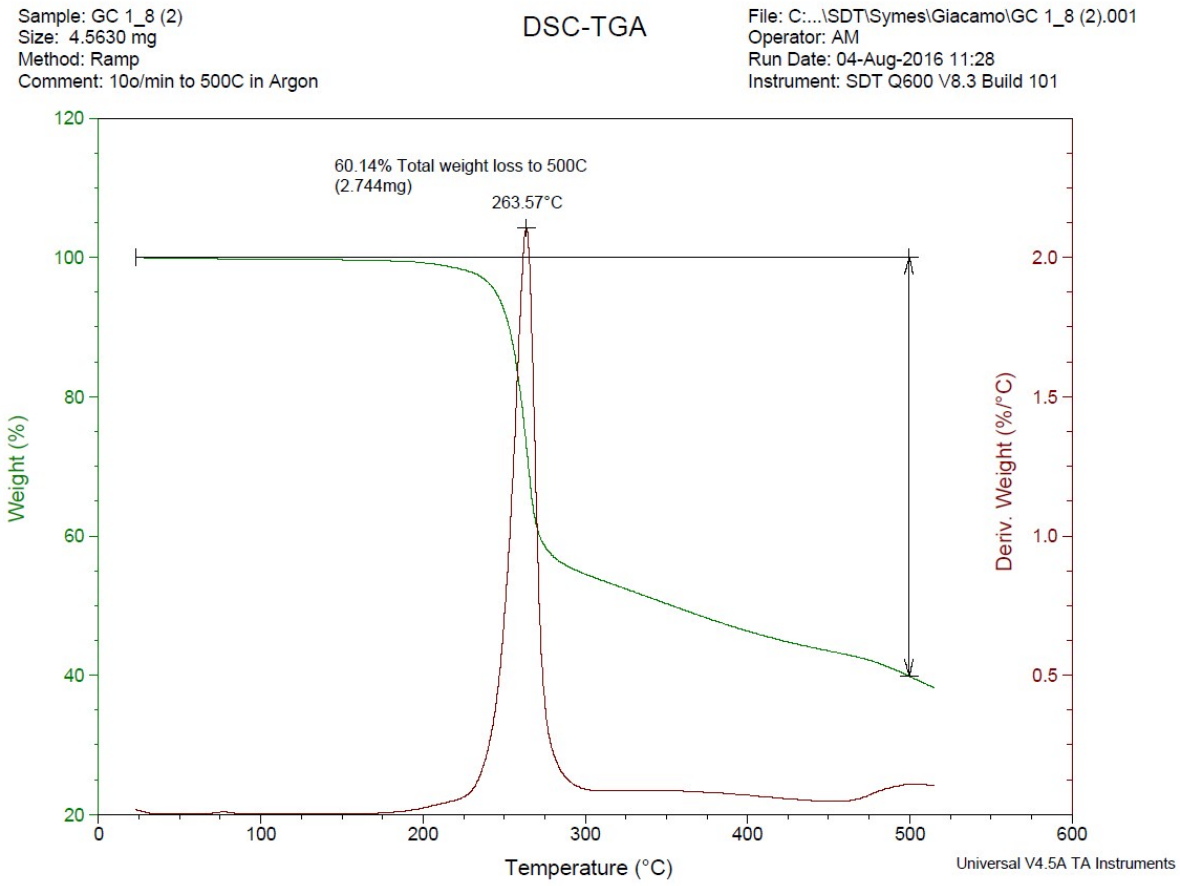

Figure S6. TGA analysis on compound **2**.

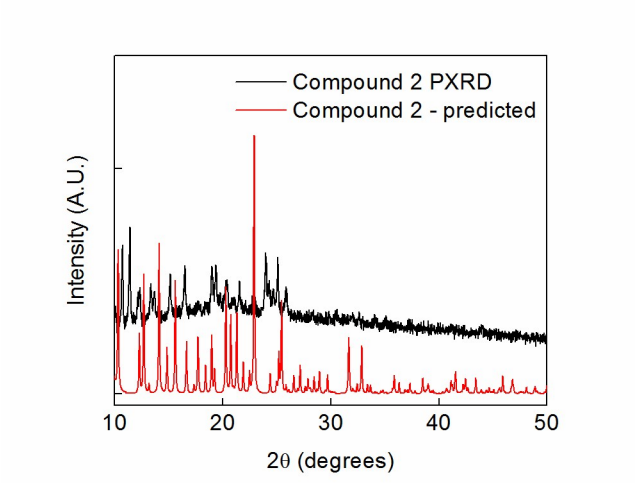

Figure S7. The PXRD pattern of compound **2**. Powder diffraction patterns were measured on **1** (Figure S3, above) and **2** (black trace in Figure S7) and compared to the pattern calculated from the single crystal structure of compound **2** (red trace in Figure S7). The three patterns do not match one another, showing that the polycrystalline samples of **1** and **2** were not crystallographically isomorphous to each other, nor indeed were they isomorphous with the crystal of **2** used for the single crystal measurement. This is not surprising given that it was observed that two morphologies of crystals were present in the sample used for the single crystal measurement – rods and plates (see discussion of the single crystal data below). Single crystal data were collected on a plate-like crystal. Moreover, different solvates are likely to crystallise with different crystal structures, which would then have different powder patterns. Hence we conclude that the crystal forms investigated are not isomorphic. The NMR data (Figures S1, S4, S5, S8 and S9) give very strong evidence, however, that complexes **1**-**3** are isostructural at the molecular level, supporting our assertion that their solution-phase chemistry can be meaningfully compared.

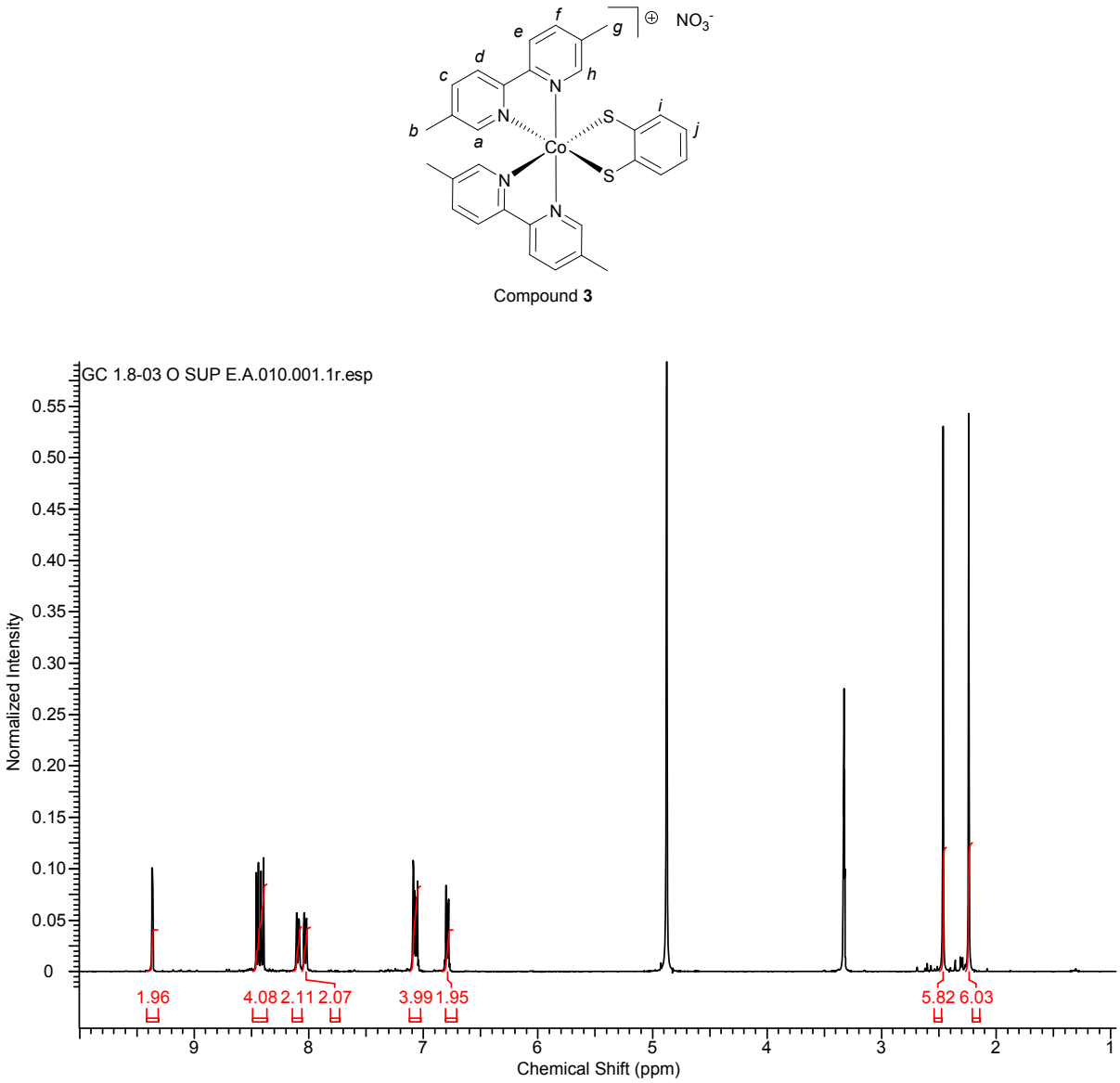

Figure S8. ^{1}H NMR spectrum of compound **3** in MeOD.

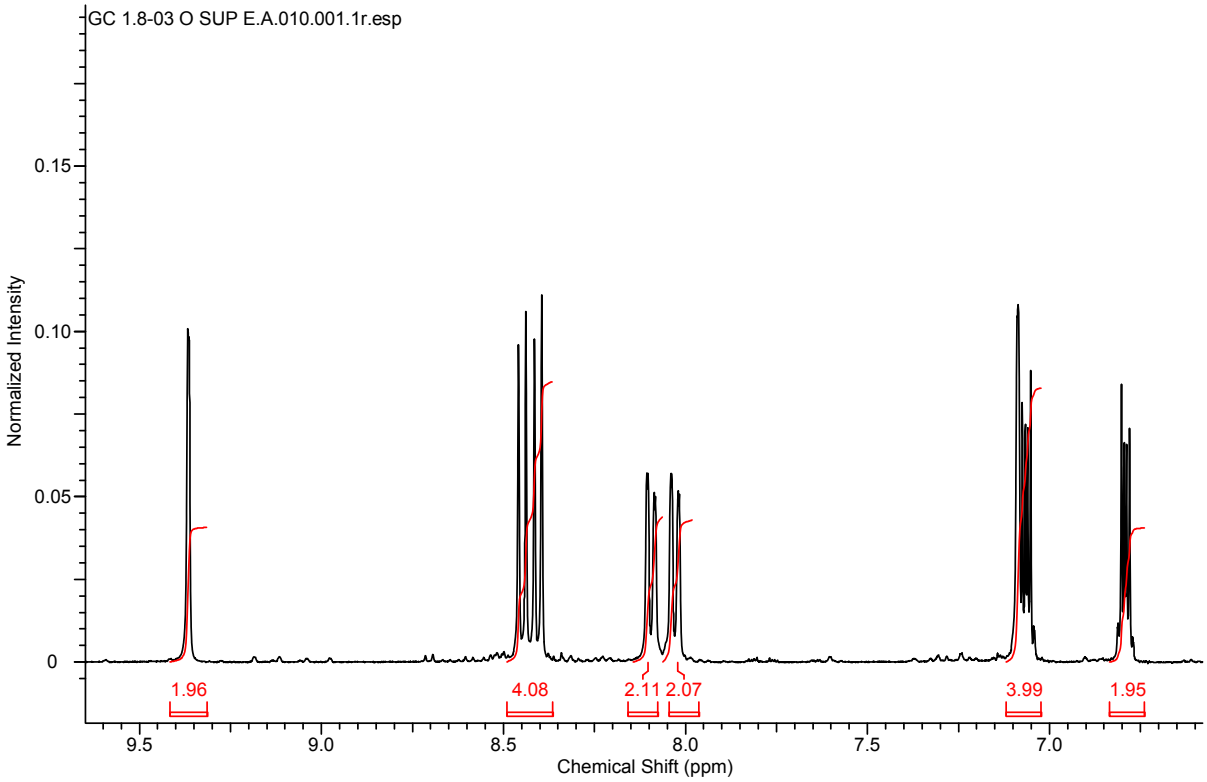

Figure S9. Expansion of the aromatic region of the ^{1}H NMR spectrum of **3** shown in Fig. S4.

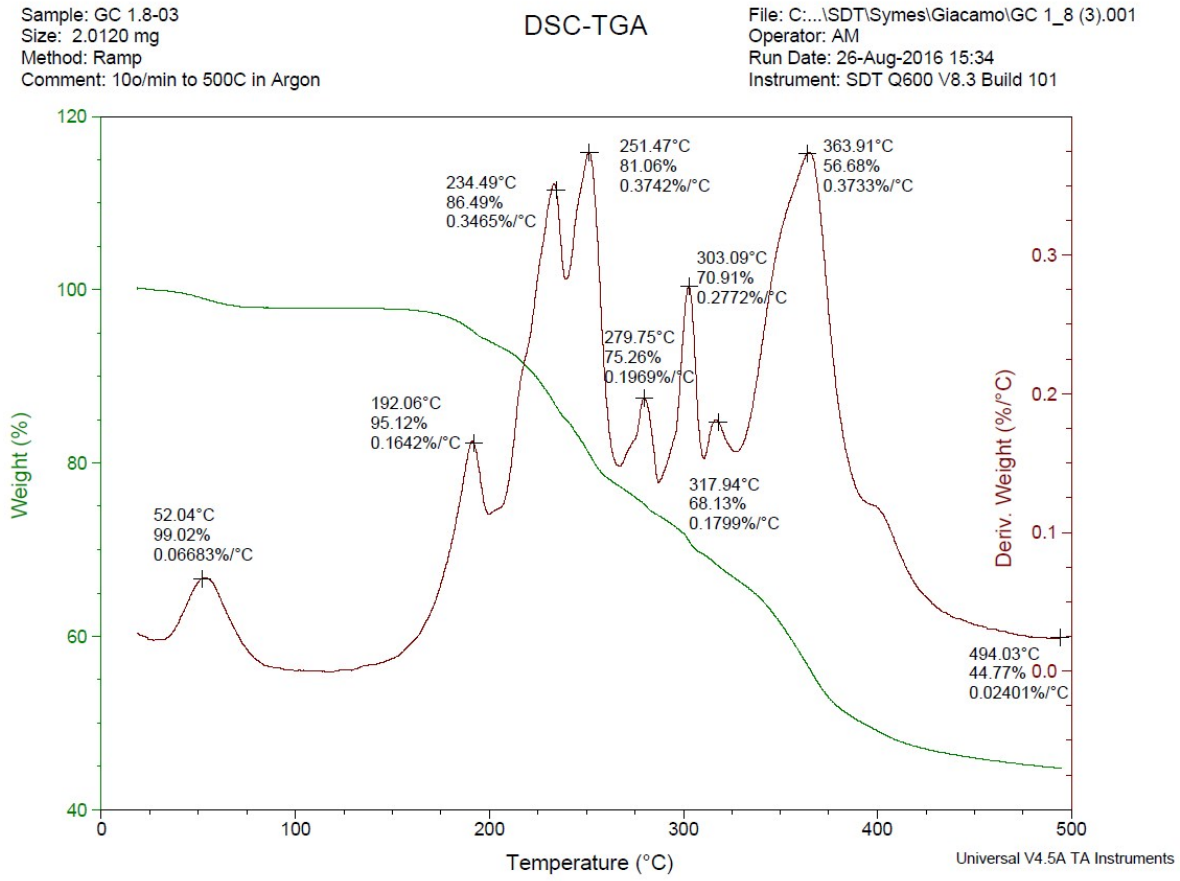

Figure S10. TGA analysis on compound **3**.

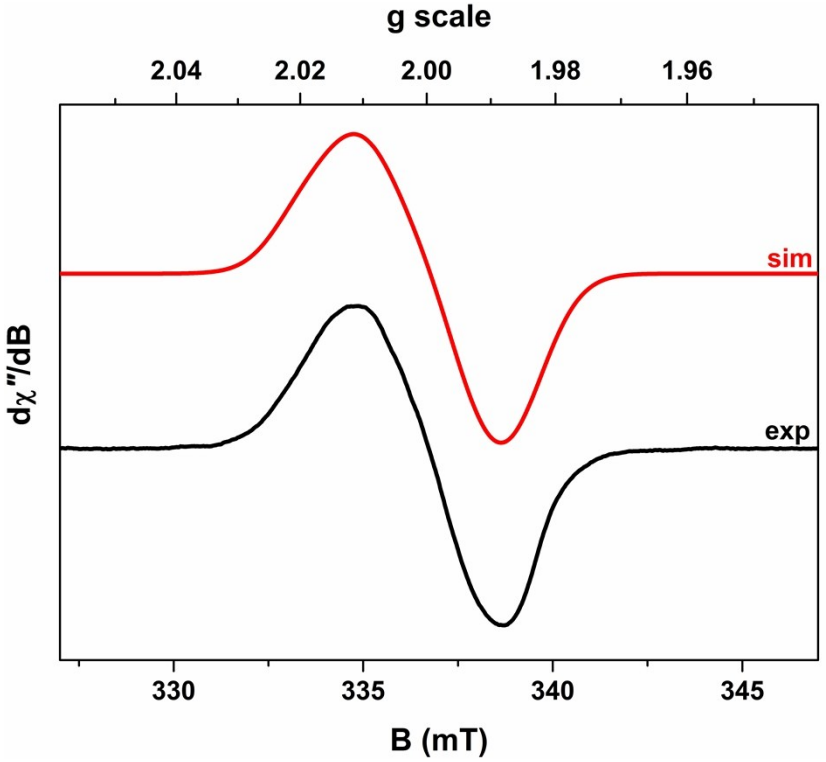

Figure S11. X-band EPR spectrum of paramagnetic species generated from the reaction of complex **2** with $NOBF_4$, recorded in acetonitrile/THF solution at 150 K (experimental conditions: frequency, 9.4243 GHz; power, 0.63 mW; modulation, 0.3 mT). Experimental data are represented by the black line; simulation is depicted by the red trace.

Supplementary Computational Methods and Results

Natural transition orbitals: When expressed in terms of canonical molecular orbitals, a particular electronic excitation often has contributions from many transitions between filled and vacant MOs. NTO analysis transforms the transitions between canonical MOs into transitions between pairs of donor/acceptor NTOs that maximally account for the excitation (by diagonalizing the transition density matrix). Very often, a single NTO pair is sufficient to characterize an excitation in terms of its orbital character.

Table S1 lists the MO transitions contributing significantly to S_1 of complex **2** and S_2 of complex **3**; the dominant NTOs are presented in the main text.

Table S1. MO transitions with >10% weight contributing to the relevant excitations of complexes **2** and **3**; H = HOMO, L = LUMO.

Complex **2**	Donor MO	Acceptor MO	Weight	Complex **3**	Donor MO	Acceptor MO	Weight
S_1	H	L + 7	26%	S_2	H	L + 4	30%
	H	L + 3	25%		H – 9	L + 4	10%
	H – 5	L + 7	13%		H	L + 6	9%
	H – 5	L + 3	10%		H – 18	L + 4	7%
					H – 7	L + 4	5%

Axis system: The complex has C_2 symmetry; by convention, the *z*-axis is taken along the C_2 axis (*i.e.*, bisecting X–Co–X, X = O or S). However, it is more convenient here to define *z* along the *trans* N–Co–N axis, with *y* along the C_2 axis. Note that with this choice, the *x*- and *y*-axes do not coincide with Co–L bonds, but bisect them; the lobes of the d_{xy} orbital therefore point towards the ligands and the d_{x2-y2} lobes point in-between.

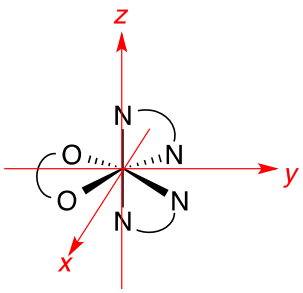

Linear fit of solvatochromic trend: The experimental excitation energies of complex **2** were used to fit a linear model of the form

$$\Delta E_{\text{pred}} = a + b\, f_{\text{O}}(\varepsilon) + c\, \alpha$$

which predicts the excitation energy, ΔE_{pred}, as a linear function of the Onsager function $f_{\text{O}}(\varepsilon) = (\varepsilon - 1)/(2\varepsilon + 1)$ and the Kamlet–Taft hydrogen-bonding strength parameter α. The fit parameters a, b, c were determined using the LinearModelFit function in *Mathematica* v. 10.3.1; quality of fit: $R^2 = 0.771$; Adjusted $R^2 = 0.694$.

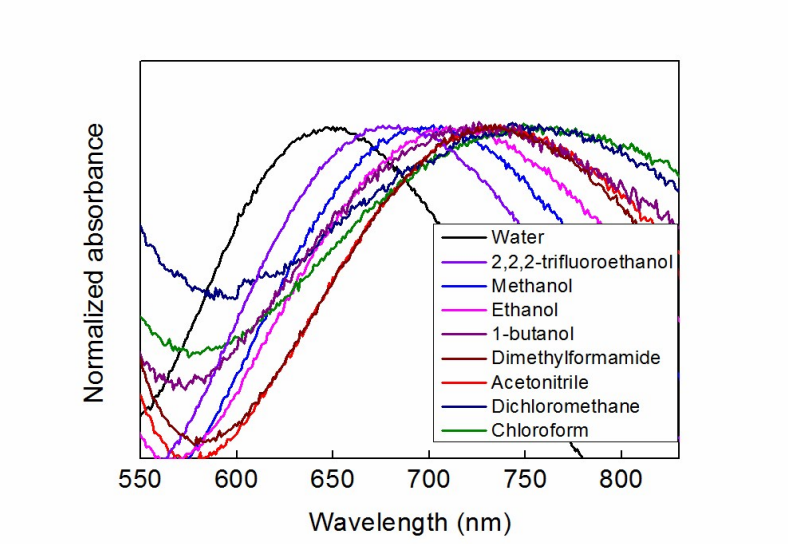

Figure S12. Plot showing an overlay of the normalized absorption profiles (in the region 550-820 nm) of compound **2** in the solvents indicated, showing how the position of λ_{max} within this range shifts. All spectra were measured at a concentration of 5 mM, except those in butanol, chloroform and dichloromethane (2.5 mM).

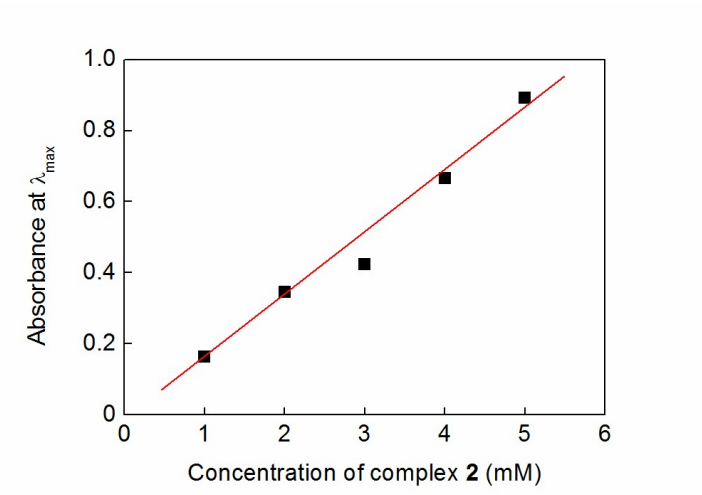

Figure S13. Absorbance of the lowest energy absorption band of compound **2** in methanol as a function of concentration. The points at concentrations of 1, 2, 4 and 5 mM were averaged to give an extinction coefficient of 171 M^{-1} cm^{-1}, with an error of ±6 M^{-1} cm^{-1}. The red line is a linear fit and is provided as a guide to the eye.

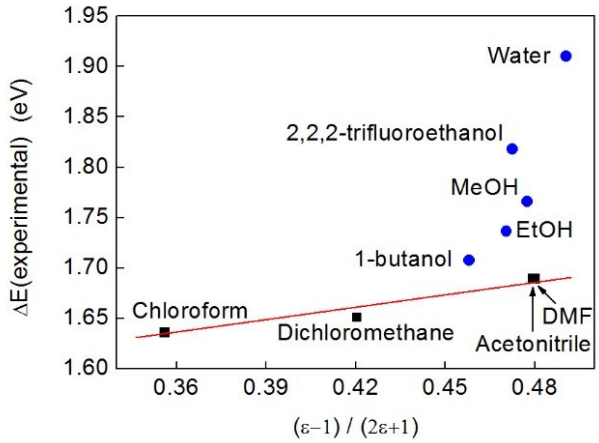

Figure S14. Plot showing the relationship between the experimentally-determined excitation energies (ΔE(experimental)) and the stabilization energy of a dipole in a spherical cavity for the various solvents probed according to Onsager's model, $f_O(\varepsilon) = (\varepsilon - 1)/(2\varepsilon + 1)$. Non hydrogen bonding solvents are depicted with black squares and the linear trend is shown as a red line as a guide to the eye. Hydrogen bonding solvents are shown as blue circles. The trend is essentially the same as that shown in Figure 5 in the main text.

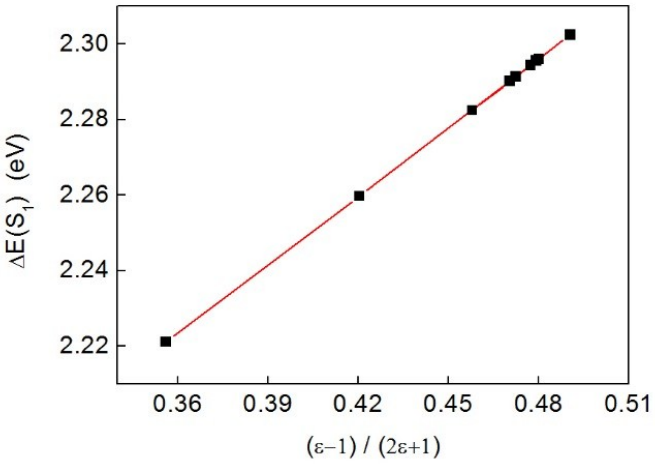

Figure S15. Plot showing the linear relationship between the excitation energies determined by TD-DFT ($\Delta E(S_1)$) and the stabilization energy of a dipole in a spherical cavity for the various solvents probed according to Onsager's model, $f_O(\varepsilon) = (\varepsilon - 1)/(2\varepsilon + 1)$.

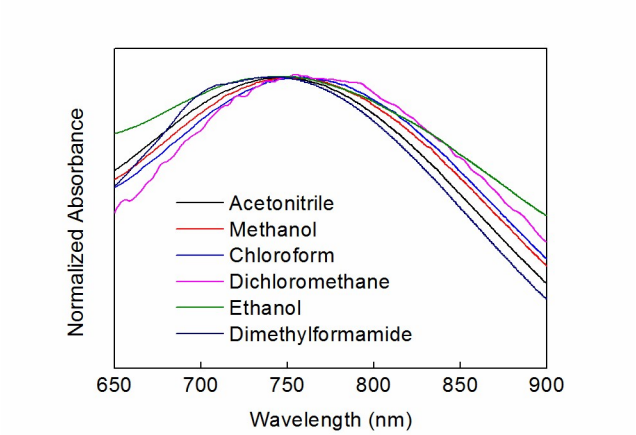

Figure S16. Plot showing an overlay of the normalized absorption profiles (in the region 650-900 nm) of compound **3** in the solvents indicated, showing how the position of λ_{max} within this range shifts. All spectra were measured at a concentration of 1.9 mM, with the exception of those taken in acetonitrile and DMF (both 1.6 mM).

Single crystal crystallographic data for complex 2 (CCDC 1452332)

Refinement

Crystal data, data collection and structure refinement details are summarized in the tables below.

Computing details

Data collection: *CrystalClear*-SM Expert 2.1 b31 (Rigaku, 2014); cell refinement: *CrysAlis PRO* 1.171.38.41 (Rigaku OD, 2015); data reduction: *CrysAlis PRO* 1.171.38.41 (Rigaku OD, 2015); program used to solve the structure: SuperFlip (Palatinus & Chapuis, 2007); program(s) used to refine structure: *SHELXL* (Sheldrick, 2015); molecular graphics: Olex2 (Dolomanov *et al.*, 2009); software used to prepare material for publication: Olex2 (Dolomanov *et al.*, 2009).

References

[S1]Dolomanov, O. V., Bourhis, L. J., Gildea, R. J., Howard, J. A. K. & Puschmann, H. (2009). *J. Appl. Cryst.* **42**, 339–341.

[S2]Sheldrick, G. M. (2015). *Acta Cryst.* C**71**, 3–8.

[S3]Palatinus, L., Chapuis, G. (2007). *J. Appl. Cryst.* **40**, 786-790.

Crystal data

$C_{30}H_{28}CoN_4O_2{\cdot}1(NO_3)$	D_x = 1.057 Mg m^{-3}
M_r = 597.50	Mo *K*α radiation, λ = 0.71075 Å
Trigonal, $P\bar{3}c1$	Cell parameters from 5011 reflections
a = 21.2619 (15) Å	θ = 2.2–25.1°
c = 14.3882 (10) Å	μ = 0.49 mm^{-1}
V = 5633.0 (7) Å^3	*T* = 100 K
Z = 6	Plate, brown
F(000) = 1860	0.06 × 0.06 × 0.01 mm

Data collection

Rigaku AFC12 (Right) diffractometer	3339 independent reflections
Radiation source: rotating anode, FR-E+ SuperBright	1325 reflections with $I > 2\sigma(I)$

Detector resolution: 28.5714 pixels mm^{-1}	R_{int} = 0.240
ω scans	θ_{max} = 25.1°, θ_{min} = 1.9°
Absorption correction: multi-scan *CrysAlis PRO* 1.171.38.41 (Rigaku Oxford Diffraction, 2015) Empirical absorption correction using spherical harmonics, implemented in SCALE3 ABSPACK scaling algorithm.	*h* = -24⟶25
T_{min} = 0.357, T_{max} = 1.000	*k* = -25⟶25
40590 measured reflections	*l* = -12⟶17

Refinement

Refinement on F^2	13 restraints
Least-squares matrix: full	Hydrogen site location: inferred from neighbouring sites
$R[F^2 > 2\sigma(F^2)]$ = 0.126	H-atom parameters constrained
$wR(F^2)$ = 0.403	$w = 1/[\sigma^2(F_o^2) + (0.2P)^2]$ where $P = (F_o^2 + 2F_c^2)/3$
S = 1.11	$(\Delta/\sigma)_{max}$ = 0.002
3339 reflections	$\Delta\rangle_{max}$ = 0.89 e $Å^{-3}$
197 parameters	$\Delta\rangle_{min}$ = -0.41 e $Å^{-3}$

Special details

Geometry. All esds (except the esd in the dihedral angle between two l.s. planes) are estimated using the full covariance matrix. The cell esds are taken into account individually in the estimation of esds in distances, angles and torsion angles; correlations between esds in cell parameters are only used when they are defined by crystal symmetry. An approximate (isotropic) treatment of cell esds is used for estimating esds involving l.s. planes.
Refinement. Overall data quality not high, probably due to large solvent accessible voids (19% of cell) and solvent loss. The electron density in the channels was accounted for using SQUEEZE which calculated a void volume of 1149 $Å^3$ containing 214 electrons which could correspond to 5 molecules of Et_2O. There are two nitrate anion sites modelled. One is 1/6 occupied and the second is disordered around a 3-fold axis. There is one central orientation with the nitrogen on the 3-fold axis which is 1/6 occupied and 3 equivalent orientations which have 2 oxygens common with the first orientation and third which lies on the 3-fold axis. Distance restraints were applied and partially occupied atoms refined with isotropic adps.

Fractional atomic coordinates and isotropic or equivalent isotropic displacement parameters (Å²)

	x	*y*	*z*	U_{iso}*/U_{eq}	Occ. (<1)
Co1	0.48521 (10)	0.48521 (10)	0.2500	0.0611 (8)	
O1	0.3985 (4)	0.4449 (4)	0.1799 (4)	0.0663 (19)	
N1	0.5275 (4)	0.5716 (5)	0.1714 (5)	0.062 (2)	
N2	0.5253 (4)	0.4489 (5)	0.1587 (5)	0.064 (2)	
C2	0.3533 (7)	0.3780 (6)	0.2113 (6)	0.070 (3)	
C3	0.2856 (6)	0.3325 (7)	0.1729 (8)	0.082 (3)	
H3	0.2698	0.3484	0.1207	0.098*	
C4	0.2403 (7)	0.2635 (7)	0.2102 (8)	0.096 (4)	
H4	0.1943	0.2322	0.1828	0.116*	
C11	0.5254 (6)	0.6322 (6)	0.1845 (6)	0.071 (3)	
H11	0.5002	0.6357	0.2370	0.085*	
C12	0.5582 (6)	0.6897 (6)	0.1250 (7)	0.078 (3)	
C13	0.5927 (6)	0.6855 (6)	0.0501 (7)	0.083 (4)	
H13	0.6146	0.7248	0.0075	0.100*	
C14	0.5963 (5)	0.6236 (7)	0.0352 (6)	0.071 (3)	
H14	0.6222	0.6204	-0.0167	0.085*	
C15	0.5620 (5)	0.5659 (6)	0.0964 (6)	0.062 (3)	
C16	0.5594 (5)	0.4963 (6)	0.0873 (6)	0.063 (3)	
C17	0.5875 (5)	0.4728 (7)	0.0141 (6)	0.073 (3)	
H17	0.6118	0.5045	-0.0365	0.088*	
C18	0.5799 (6)	0.4055 (6)	0.0157 (7)	0.075 (3)	
H18	0.5972	0.3898	-0.0350	0.090*	
C19	0.5474 (6)	0.3599 (7)	0.0897 (7)	0.078 (3)	
C20	0.5210 (6)	0.3850 (7)	0.1600 (6)	0.068 (3)	
H20	0.4985	0.3543	0.2120	0.082*	
C21	0.5497 (8)	0.7563 (6)	0.1430 (8)	0.118 (5)	
H21A	0.4998	0.7403	0.1625	0.177*	

H21B	0.5606	0.7851	0.0860	0.177*	
H21C	0.5834	0.7861	0.1922	0.177*	
C22	0.5397 (8)	0.2863 (7)	0.0940 (8)	0.102 (4)	
H22A	0.5719	0.2856	0.1422	0.153*	
H22B	0.5528	0.2746	0.0337	0.153*	
H22C	0.4893	0.2503	0.1089	0.153*	
O10N	0.862 (2)	0.732 (3)	0.033 (3)	0.15 (2)*	0.1667
O11N	0.7705 (17)	0.669 (2)	0.122 (2)	0.067 (11)*	0.1666
O12N	0.866 (2)	0.662 (3)	0.137 (4)	0.14 (2)*	0.1667
N10N	0.8335 (16)	0.6894 (17)	0.098 (2)	0.11 (2)*	0.1667
O1N	0.3677 (6)	0.6302 (6)	0.2000 (8)	0.106 (4)*	0.7221
O2N	0.3333	0.6667	0.0961 (14)	0.156 (9)*	0.8333
N1N	0.3333	0.6667	0.1992 (17)	0.034 (6)*	0.1666
N2N	0.3199 (6)	0.6405 (8)	0.1753 (12)	0.034 (6)*	0.2778

Atomic displacement parameters (Å²)

	U^{11}	U^{22}	U^{33}	U^{12}	U^{13}	U^{23}
Co1	0.0788 (12)	0.0788 (12)	0.0266 (10)	0.0401 (12)	-0.0038 (4)	0.0038 (4)
O1	0.077 (5)	0.075 (5)	0.037 (4)	0.030 (4)	-0.009 (3)	0.004 (3)
N1	0.081 (6)	0.075 (6)	0.025 (4)	0.035 (5)	-0.007 (4)	0.008 (4)
N2	0.082 (6)	0.080 (6)	0.032 (4)	0.041 (5)	-0.010 (4)	-0.005 (4)
C2	0.086 (8)	0.082 (8)	0.043 (6)	0.043 (7)	0.002 (6)	0.001 (5)
C3	0.081 (9)	0.098 (9)	0.063 (7)	0.044 (8)	-0.007 (6)	0.002 (7)
C4	0.087 (9)	0.094 (9)	0.093 (9)	0.034 (8)	-0.030 (7)	-0.007 (8)
C11	0.116 (9)	0.061 (7)	0.035 (5)	0.043 (7)	-0.010 (5)	0.000 (5)
C12	0.124 (10)	0.063 (7)	0.035 (6)	0.038 (7)	0.001 (6)	-0.001 (5)
C13	0.115 (10)	0.068 (8)	0.038 (6)	0.025 (7)	-0.018 (6)	0.006 (5)
C14	0.069 (7)	0.094 (9)	0.030 (5)	0.026 (7)	-0.012 (5)	-0.005 (6)
C15	0.074 (7)	0.064 (7)	0.030 (5)	0.023 (6)	-0.008 (5)	0.004 (5)
C16	0.050 (6)	0.091 (8)	0.033 (6)	0.025 (6)	-0.007 (5)	0.006 (5)
C17	0.061 (7)	0.126 (10)	0.025 (5)	0.041 (7)	-0.005 (4)	0.012 (6)
C18	0.122 (10)	0.091 (9)	0.046 (6)	0.078 (8)	-0.024 (6)	-0.011 (6)
C19	0.111 (9)	0.109 (9)	0.039 (6)	0.075 (8)	-0.016 (6)	-0.004 (6)
C20	0.093 (8)	0.087 (9)	0.032 (5)	0.051 (7)	-0.007 (5)	0.001 (5)
C21	0.200 (15)	0.074 (8)	0.060 (7)	0.054 (9)	-0.003 (9)	0.003 (6)

C22	0.183 (13)	0.128 (11)	0.055 (7)	0.123 (10)	0.000 (8)	0.000 (7)

*Geometric parameters (Å, º) for complex **2***

Co1—O1	1.889 (6)	C17—C18	1.359 (14)
Co1—O1^{i}	1.889 (6)	C18—H18	0.9500
Co1—N1	1.951 (8)	C18—C19	1.371 (14)
Co1—N1^{i}	1.951 (8)	C19—C20	1.387 (13)
Co1—N2	1.926 (8)	C19—C22	1.491 (15)
Co1—N2^{i}	1.926 (8)	C20—H20	0.9500
O1—C2	1.335 (11)	C21—H21A	0.9800
N1—C11	1.325 (11)	C21—H21B	0.9800
N1—C15	1.344 (11)	C21—H21C	0.9800
N2—C16	1.366 (11)	C22—H22A	0.9800
N2—C20	1.315 (12)	C22—H22B	0.9800
C2—C2^{i}	1.439 (19)	C22—H22C	0.9800
C2—C3	1.386 (13)	O10N—N10N	1.239 (10)
C3—H3	0.9500	O11N—N10N	1.231 (10)
C3—C4	1.400 (14)	O12N—N10N	1.238 (10)
C4—C4^{i}	1.43 (2)	O1N—N1N	1.306 (7)
C4—H4	0.9500	O1N—N2N^{ii}	1.198 (9)
C11—H11	0.9500	O1N—N2N^{iii}	1.823 (17)
C11—C12	1.365 (13)	O1N—N2N	1.197 (9)
C12—C13	1.332 (14)	O2N—N2N^{iii}	1.238 (10)
C12—C21	1.535 (16)	O2N—N2N	1.238 (10)
C13—H13	0.9500	O2N—N2N^{ii}	1.238 (10)
C13—C14	1.372 (15)	N1N—O1N^{iii}	1.306 (7)
C14—H14	0.9500	N1N—O1N^{ii}	1.306 (7)
C14—C15	1.385 (13)	N2N—O1N^{iii}	1.198 (9)
C15—C16	1.458 (14)	N2N—O1N^{ii}	1.823 (17)
C16—C17	1.419 (14)	N2N—N2N^{ii}	0.84 (3)
C17—H17	0.9500	N2N—N2N^{iii}	0.84 (3)
O1—Co1—O1^{i}	88.8 (4)	C18—C17—C16	120.6 (10)

O1^{i}—Co1—N1^{i}	90.2 (3)	C18—C17—H17	119.7
O1—Co1—N1	90.2 (3)	C17—C18—H18	119.6
O1—Co1—N1^{i}	176.6 (3)	C17—C18—C19	120.7 (10)
O1^{i}—Co1—N1	176.6 (3)	C19—C18—H18	119.6
O1—Co1—N2^{i}	92.8 (3)	C18—C19—C20	116.9 (10)
O1—Co1—N2	88.9 (3)	C18—C19—C22	121.8 (10)
O1^{i}—Co1—N2	92.8 (3)	C20—C19—C22	121.4 (11)
O1^{i}—Co1—N2^{i}	88.9 (3)	N2—C20—C19	123.6 (10)
N1—Co1—N1^{i}	91.0 (4)	N2—C20—H20	118.2
N2^{i}—Co1—N1^{i}	83.9 (4)	C19—C20—H20	118.2
N2—Co1—N1	83.9 (4)	C12—C21—H21A	109.5
N2—Co1—N1^{i}	94.4 (3)	C12—C21—H21B	109.5
N2^{i}—Co1—N1	94.4 (3)	C12—C21—H21C	109.5
N2^{i}—Co1—N2	177.6 (5)	H21A—C21—H21B	109.5
C2—O1—Co1	108.9 (6)	H21A—C21—H21C	109.5
C11—N1—Co1	127.5 (7)	H21B—C21—H21C	109.5
C11—N1—C15	119.1 (9)	C19—C22—H22A	109.5
C15—N1—Co1	113.3 (7)	C19—C22—H22B	109.5
C16—N2—Co1	113.2 (7)	C19—C22—H22C	109.5
C20—N2—Co1	126.0 (7)	H22A—C22—H22B	109.5
C20—N2—C16	120.7 (9)	H22A—C22—H22C	109.5
O1—C2—C2^{i}	116.8 (5)	H22B—C22—H22C	109.5
O1—C2—C3	123.5 (9)	O11N—N10N—O10N	120.8 (13)
C3—C2—C2^{i}	119.7 (7)	O11N—N10N—O12N	118.9 (13)
C2—C3—H3	119.7	O12N—N10N—O10N	120.0 (13)
C2—C3—C4	120.6 (10)	N2N—O1N—N2N^{iii}	21.6 (8)
C4—C3—H3	119.7	N2N^{ii}—O1N—N2N^{iii}	21.6 (8)
C3—C4—C4^{i}	119.7 (6)	N2N—O1N—N2N^{ii}	40.8 (14)
C3—C4—H4	120.2	N2N^{iii}—O2N—N2N	39.4 (13)
C4^{i}—C4—H4	120.2	N2N^{iii}—O2N—N2N^{ii}	39.4 (13)
N1—C11—H11	118.9	N2N—O2N—N2N^{ii}	39.4 (13)
N1—C11—C12	122.2 (10)	O1N^{iii}—N1N—O1N^{ii}	119.99 (4)
C12—C11—H11	118.9	O1N^{iii}—N1N—O1N	119.99 (4)
C11—C12—C21	118.5 (11)	O1N^{ii}—N1N—O1N	119.99 (4)
C13—C12—C11	119.9 (10)	O1N—N2N—O1N^{ii}	94.7 (9)

C13—C12—C21	121.5 (11)	O1N—N2N—O1N^{iii}	141.5 (17)
C12—C13—H13	120.4	O1N^{iii}—N2N—O1N^{ii}	94.7 (9)
C12—C13—C14	119.2 (10)	O1N—N2N—O2N	109.3 (10)
C14—C13—H13	120.4	O1N^{iii}—N2N—O2N	109.2 (10)
C13—C14—H14	120.2	O2N—N2N—O1N^{ii}	78.3 (11)
C13—C14—C15	119.5 (10)	N2N^{ii}—N2N—O1N^{iii}	126.5 (11)
C15—C14—H14	120.2	N2N^{ii}—N2N—O1N	69.7 (12)
N1—C15—C14	120.0 (10)	N2N^{iii}—N2N—O1N^{ii}	31.9 (6)
N1—C15—C16	114.7 (9)	N2N^{iii}—N2N—O1N^{iii}	69.5 (12)
C14—C15—C16	125.3 (10)	N2N^{iii}—N2N—O1N	126.6 (11)
N2—C16—C15	114.8 (9)	N2N^{ii}—N2N—O1N^{ii}	31.8 (6)
N2—C16—C17	117.4 (10)	N2N^{iii}—N2N—O2N	70.3 (7)
C17—C16—C15	127.9 (10)	N2N^{ii}—N2N—O2N	70.3 (7)
C16—C17—H17	119.7	N2N^{iii}—N2N—N2N^{ii}	60.000 (10)
Co1—O1—C2—C2^{i}	1.5 (13)	C15—N1—C11—C12	-1.1 (15)
Co1—O1—C2—C3	-177.9 (9)	C15—C16—C17—C18	-179.3 (9)
Co1—N1—C11—C12	179.0 (8)	C16—N2—C20—C19	-2.4 (14)
Co1—N1—C15—C14	-178.4 (7)	C16—C17—C18—C19	-2.5 (15)
Co1—N1—C15—C16	1.6 (10)	C17—C18—C19—C20	2.2 (15)
Co1—N2—C16—C15	2.9 (10)	C17—C18—C19—C22	-178.8 (10)
Co1—N2—C16—C17	-176.9 (6)	C18—C19—C20—N2	0.3 (15)
Co1—N2—C20—C19	176.3 (8)	C20—N2—C16—C15	-178.2 (8)
O1^{i}—Co1—O1—C2	-0.5 (5)	C20—N2—C16—C17	2.0 (12)
O1—C2—C3—C4	-178.9 (10)	C21—C12—C13—C14	-177.5 (10)
N1—Co1—O1—C2	176.2 (6)	C22—C19—C20—N2	-178.7 (10)
N1—C11—C12—C13	1.1 (17)	N2N^{ii}—O1N—N2N—O1N^{iii}	-124 (2)
N1—C11—C12—C21	177.1 (10)	N2N^{iii}—O1N—N2N—O1N^{iii}	-104 (3)
N1—C15—C16—N2	-3.0 (11)	N2N^{iii}—O1N—N2N—O1N^{ii}	0.0 (4)
N1—C15—C16—C17	176.8 (8)	N2N^{ii}—O1N—N2N—O1N^{ii}	-20.0 (10)
N2—Co1—O1—C2	92.3 (6)	N2N^{iii}—O1N—N2N—O2N	79.3 (13)
N2^{i}—Co1—O1—C2	-89.4 (6)	N2N^{ii}—O1N—N2N—O2N	59.3 (12)
N2—C16—C17—C18	0.4 (13)	N2N^{ii}—O1N—N2N—N2N^{iii}	-20.0 (10)
C2^{i}—C2—C3—C4	1.7 (19)	N2N^{iii}—O1N—N2N—N2N^{ii}	20.0 (10)
C2—C3—C4—C4^{i}	1 (2)	N2N^{iii}—O2N—N2N—O1N^{ii}	-32.1 (7)

C11—N1—C15—C14	1.6 (13)	N2N^{ii}—O2N—N2N—O1N^{iii}	123.0 (13)
C11—N1—C15—C16	-178.4 (8)	N2N^{iii}—O2N—N2N—O1N	-123.1 (13)
C11—C12—C13—C14	-1.6 (17)	N2N^{iii}—O2N—N2N—O1N^{iii}	58.8 (15)
C12—C13—C14—C15	2.2 (15)	N2N^{ii}—O2N—N2N—O1N	-58.9 (15)
C13—C14—C15—N1	-2.2 (14)	N2N^{ii}—O2N—N2N—O1N^{ii}	32.0 (7)
C13—C14—C15—C16	177.8 (9)	N2N^{ii}—O2N—N2N—N2N^{iii}	64.2 (3)
C14—C15—C16—N2	177.0 (8)	N2N^{iii}—O2N—N2N—N2N^{ii}	-64.2 (3)
C14—C15—C16—C17	-3.2 (15)		

Symmetry codes: (i) *y*, *x*, -*z*+1/2; (ii) -*y*+1, *x*-*y*+1, *z*; (iii) -*x*+*y*, -*x*+1, *z*.

Document origin: *publCIF* [Westrip, S. P. (2010). *J. Appl. Cryst.*, **43**, 920-925].[S4]

References

S1 O. V. Dolomanov, L. J. Bourhis, R. J. Gildea, J. A. K. Howard and H. Puschmann, *J. Appl. Cryst.* 2009, **42**, 339.

S2 G. M. Sheldrick, *Acta Cryst.* C, 2015, **71**, 3.

S3 L. Palatinus, G. Chapuis, *J. Appl. Cryst.* 2007, **40**, 786-790.

S4 S. P. Westrip, *J. Appl. Cryst.* 2010, **43**, 920.